Composites Science and Technology 251 (2024) 110564

Contents lists available at ScienceDirect

Composites Science and Technology

journal homepage: www.elsevier.com/locate/compscitech

Influence of rapid high-temperature processing on the interface of CF/PEEK, a quick and effective method for enhancing the IFSS

Dimitrios Gaitanelis [a,b,*], Chris Worrall [c], Mihalis Kazilas [d]

[a] Advanced Manufacturing Research Centre with Boeing, University of Sheffield, Catcliff, Rotherham, S60 5TZ, UK
[b] NSIRC, TWI Ltd, Granta Park, Great Abington, Cambridge, CB21 6AL, UK
[c] Advanced Composites and Adhesives Section, TWI Ltd, Cambridge, CB21 6AL, UK
[d] Brunel Composites Centre, Brunel University London, London, UB8 3PH, UK

ARTICLE INFO

Handling Editor: Marino Quaresimin

Keywords:
Poly(ether ether ketone)
A. Carbon fibres
B. Interfacial strength
B. Debonding
E. Heat treatment

ABSTRACT

This study explores the effect of rapid high-temperature processing on the interface of carbon fibre (CF) reinforced poly-ether-ether-ketone (PEEK). Specimens that have been thermally treated at slower and faster heating rates and specimens that have not been post-manufacturing treated (virgin) are examined with single fibre pull-out tests. A comparison between their interfacial shear strength (IFSS) and their failure modes takes place. Scanning electron microscopy is used to assess the surface morphology of the thermally treated specimens, and partly cross-polarised microscopy is employed to investigate the development of transcrystallinity. Furthermore, to identify the extent of thermal degradation the specimens are examined with attenuated total reflection Fourier transform infrared spectroscopy. At faster heating rates, an improved interfacial adhesion up to 25% is found at temperatures where a low-level thermal damage is induced. At higher temperatures and despite the increased thermal damage, an IFSS increase of up to 10% is still identified. This is due to the beneficial formation of thermal residual stresses upon high-temperature processing, and overall, especially rapid high-temperature processing could effectively serve for enhancing the interface properties of CF/PEEK.

1. Introduction

The recyclability of thermoplastic composites as well as their reprocessing and fast manufacturing capabilities are some of their main benefits that contribute to sustainable aviation [1]. Especially carbon fibre (CF) reinforced poly-ether-ether-ketone (PEEK), with a service temperature above 250 °C and a good combination of mechanical properties and chemical resistance, is commonly considered for high-performance applications [2,3]. To fully exploit the benefits of CF/PEEK composites, out-of-autoclave (OOA) manufacturing methods such as laser-assisted tape placement (LATP) are increasingly studied in recent years [4–7]. In these applications, a laser heat source is used, and high temperatures are applied for a short time until consolidation is achieved without needing a post-processing autoclave treatment. This makes the manufacturing process energy- and cost-effective, but the fast cooling that takes place can result in low crystallinity content and poor mechanical performance.

To counteract these phenomena, laser repass and post-manufacturing tempering treatments are commonly employed [8–12]. For example, post-manufacturing tempering was recently applied in thermoplastic composites made with LATP and the polymer tensile strength increased by up to 32% [9]. Additionally, it was recently shown that the crystallinity of PEEK is not significantly affected when the material is heated at faster heating rates up to temperatures where a small-level thermal damage is induced [13]. This demonstrates the benefits of rapid high-temperature processing as a post-processing thermal treatment, and therefore it is important to investigate the response of CF/PEEK in these conditions.

A research question that has not been examined yet is the response of the CF/PEEK interface in rapid high-temperature processing and upon the event of thermal degradation. The interface is responsible for transferring the loads from the matrix to the fibres [14] and the resulting stress transfer efficiency plays a significant role in the ultimate mechanical properties of CF reinforced polymers (CFRPs) [15,16]. To improve the interface of CF/PEEK, most of the studies either alter the sizing agent of the CFs [17–23] or implement carbon nanotubes (CNTs) in the PEEK matrix [2,24,25]. Although these methods are effective, their implementation in industrial manufacturing scenarios can be

* Corresponding author. Advanced Manufacturing Research Centre with Boeing, University of Sheffield, Catcliff, Rotherham, S60 5TZ, UK.
E-mail address: d.gaitanelis@sheffield.ac.uk (D. Gaitanelis).

https://doi.org/10.1016/j.compscitech.2024.110564
Received 14 December 2023; Received in revised form 19 March 2024; Accepted 21 March 2024
Available online 22 March 2024

demanding and alternative methodologies should also be considered. This study addresses this gap by investigating the impact of rapid high-temperature processing on the CF/PEEK interface. Given the growing application of such processing conditions, particularly in aerospace, and their potential to enhance the overall performance of thermoplastics, gaining an in-depth understanding of their effect on the CF/PEEK interface can offer valuable insights.

To do so, in this work CF/PEEK specimens that have been post-manufacturing tempered at slower and faster heating rates are examined with single fibre pull-out tests (SFPTs). Through this process, the effect of rapid high-temperature processing on the interfacial shear stress (IFSS) and on the failure modes of CF/PEEK is assessed. Scanning electron microscopy (SEM), partly cross-polarised microscopy, and attenuated total reflection-Fourier transform infrared (ATR-FTIR) spectroscopy are also applied to examine the surface morphology, the development of transcrystallinity (TC), and the extent of thermal degradation respectively. In summary, section 2 presents the experimental process, section 3 discusses the results of each investigation and section 4 gathers the main conclusions of this work.

2. Experimental

2.1. Materials

High-strength commercial T700SC-12000-50C CFs are used in this study provided by Sigmatex Ltd., UK with a fibre diameter equal to 7.27 ± 0.32 μm. To remove the fibre's sizing agent, the as-received fibres are thermally treated at 380 °C for 7 minutes [26]. The PEEK matrix is provided by Victrex plc and particularly APTIV® 2000-012G PEEK film of 12 μm thickness is used to prepare the single fibre composites. This film has a glass transition temperature (T_g) equal to 143 °C, a melting point (T_m) of 325 °C and when it is processed at temperatures above its T_g it is capable to crystallise [27].

2.2. Specimen preparation

So far, there has not been a standard methodology for preparing samples with a thermoplastic matrix for single fibre pull-out or microbond tests, but overall, a similar procedure is followed in each research group with slight variations [28]. To manufacture the SFPT specimens of this work, two rectangular PEEK sheets are placed on a baseplate with a single CF filament positioned between them (Fig. 1). Adhesive tape is used to secure the two ends of the CF and dead weight (100g) is placed across its length to ensure the fibre's wetting during melting (Fig. 1a). This process takes place at room temperature and as soon as the setup is ready, the hot plate is set at 380 °C for 7 minuntes. This duration was found sufficient for ensuring the fibre wetting without inducing thermal degradation in the produced samples (section 3.5). The single CF/PEEK specimens are then removed from the baseplate and let to naturally cool down to room temperature (Fig. 1b). Considering that at fast manufacturing technologies, the fast heating is followed by an uncontrolled cooling process [29], natural cooling is also used in this work. In LATP studies this natural cooling has been estimated to be more than 333 °C/s [30,31], and in this work it was estimated around 1500 °C/min which overall has a negative impact on the crystallinity of CF/PEEK [29]. To examine the wetting of the CF, optical microscopy (OM) is used and to cut the specimens to lengths appropriate for testing, a Stanley thin blade (30 μm) is employed. After successfully completing these steps, the embedded fibre length (L_e) of the specimen is measured with OM and the specimens are then ready for mounting and testing (Fig. 1d).

2.3. Applied heating programs

To examine the interfacial response of CF/PEEK in rapid high-temperature processing, single fibre specimens are prepared as described in section 2.2 and are then heated in static air conditions up to 460 °C and 500 °C at 5 °C/min and 100 °C/min. This takes place with a calibrated Mettler Toledo furnace, commonly used for

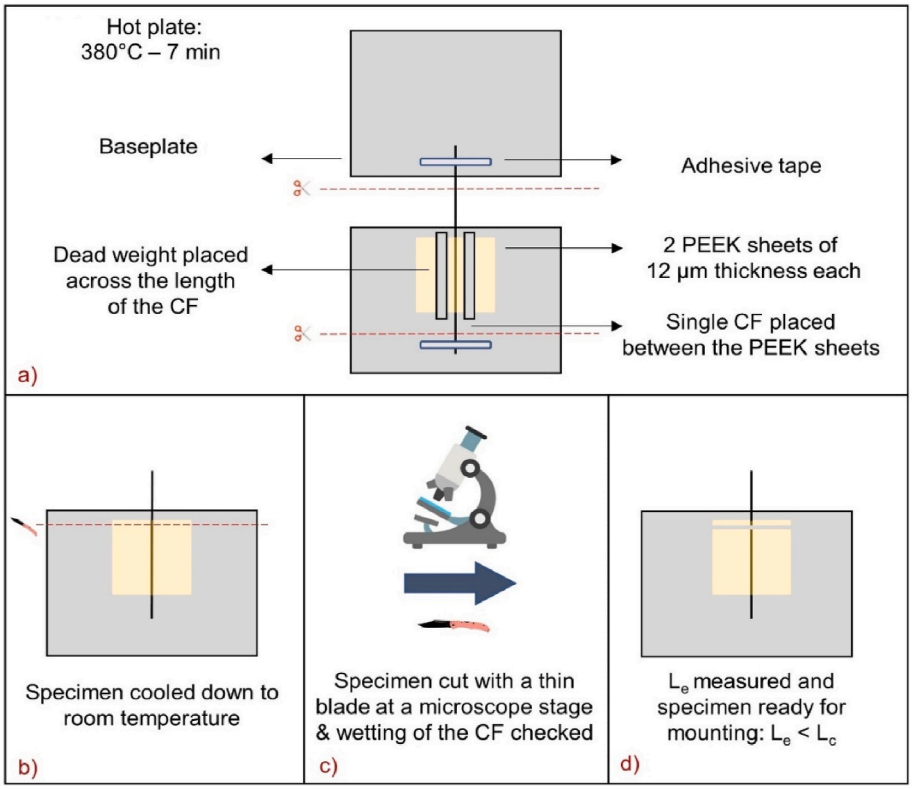

Fig. 1. Specimen preparation schematic: a, b) manufacturing, c) optical microscopy, and d) final specimen.

thermogravimetric analysis (TGA). The heating rate and the end temperature is set by the user, and the overall heating program (temperature-time) is recorded and controlled with the thermal analysis instruments, ensuring the accuracy in the applied heating rates. After the applied heating programs and similarly to the non-post treated specimens, the thermally treated samples are naturally cooled down to room temperature and are then tested with SFPTs in ambient conditions.

2.4. Single fibre pull-out tests

To perform the SFPTs, DAGE 4000 Plus supplied by Nordson DAGE Ltd., UK is used provided with a 100 g pull cartridge that can deliver a maximum load of approximately 1 N (Fig. 2). The baseplate is mounted at the stiff part of the testing equipment, while a card tab is clamped at the moving part using a set of pneumatic tweezers. Once the specimen is in position, its free fibre length is secured at the card tab with a thin layer of cyanoacrylate glue. After mounting the baseplate, an industrial camera provided by IDS Imaging Development System Ltd., UK is used to assess and improve the specimen's alignment with the load cell (Fig. 2c). To perform the pull-out tests, a displacement rate equal to 0.1 mm/min is applied and the load-displacement response is captured. The main outcome of the performed SFPTs is the value of IFSS, which is the predominantly examined property for characterising the fibre-matrix interface at CFRPs [15,28]. The value of IFSS is calculated by

$$IFSS = \frac{F_{max}}{\pi D_f L_e} \quad (1)$$

where F_{max} is the maximum load that occurs in debonding while the values of the embedded fibre length, L_e, and of the fibre diameter, D_f, are defined with the applied microscopy methods.

2.5. Microscopy characterization methods

To understand the mechanisms that affect the interfacial adhesion of CF/PEEK at the examined heating conditions, several microscopy methods are applied. OM is used to examine the failure modes that take place in the untreated and the thermally treated single CF/PEEK specimens, while their surface morphology is assessed with SEM. SEM is particularly employed to investigate the occurrence of thermal residual stresses in CF/PEEK before and after the applied high-temperature processing. Finally, to examine the development of TC partly cross-polarised microscopy is applied.

2.6. ATR-FTIR

ATR-FTIR is employed in this study to identify the extent of thermal damage that is induced in CF/PEEK at the examined heating conditions. The applied methodology has been presented in a previous study conducted by the authors, where the intensity of a new peak at 1711 cm^{-1} was correlated with the resulting extent of thermal degradation after heating PEEK and CF/PEEK at slower and faster heating rates [13]. Overall, a Nicolet iS50 FTIR spectrometer operating with a diamond ATR from Thermo Fischer Scientific Inc. is used and the spectra are collected with 128 scans and a resolution of 4 cm^{-1}. Five measurements take place for each specimen and the spectra are baseline-corrected and normalised to the 1593 cm^{-1} peak [13]. Through this process, the main spectral changes that occur in the examined single CF/PEEK specimens after the applied thermal treatments are identified and the extent of thermal degradation that takes place in each group is correlated with the resulting IFSS.

3. Results and discussion

3.1. Interfacial properties of the virgin and thermally treated specimens

To examine the interface of CF/PEEK, non-post treated (virgin) single fibre composites are initially tested. Within the examined specimens, the embedded fibre length ranged between 30 and 210 μm and successful pull-out occurred in specimens that had a value of L_e between 65 μm and 166 μm. In the examined "virgin" group, an average IFSS of 43.2 MPa ± 5.9 MPa is captured, which agrees with the results of previous researchers that examined the interfacial adhesion of PEEK with T700SC CFs [2,23,26].

Fig. 3 shows the typical load-displacement curve of a successful SFPT, capturing the characteristic interface failure upon fibre-matrix debonding that is noticed in the non-post treated and thermally treated specimens of this work. It should be mentioned that the fracture behaviour in single fibre specimens upon SFPTs is a complex matter [32,33]. Especially in CF/PEEK, the stress distribution in the interface and the interphase region – the region in the vicinity of the fibre - can be affected by several factors, including the interaction of the constituents, the presence of TC, the capability of the CF to act as a nucleation factor, and the applied manufacturing conditions [32,33]. In this study, a rounding of the peak tip is observed in the examined load-displacement curves, indicative of a ductile failure (Fig. 3). This ductile response is attributed to the predominantly amorphous matrix - resulting from the applied heating and cooling conditions examined in this work. This is also captured by the TC investigation (Fig. 13), where a relatively amorphous boundary layer is noticed in the examined samples. This

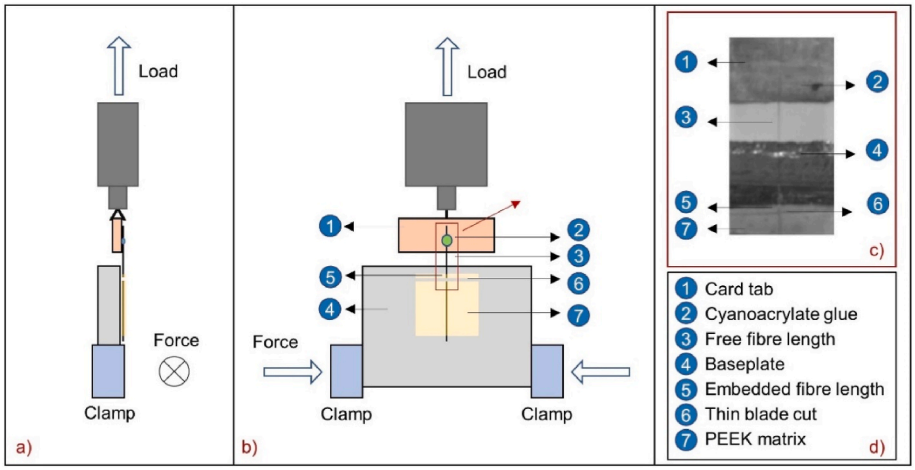

Fig. 2. Single fibre pull-out test schematic: a) side view, b) front view, c) detail from the test, and d) index.

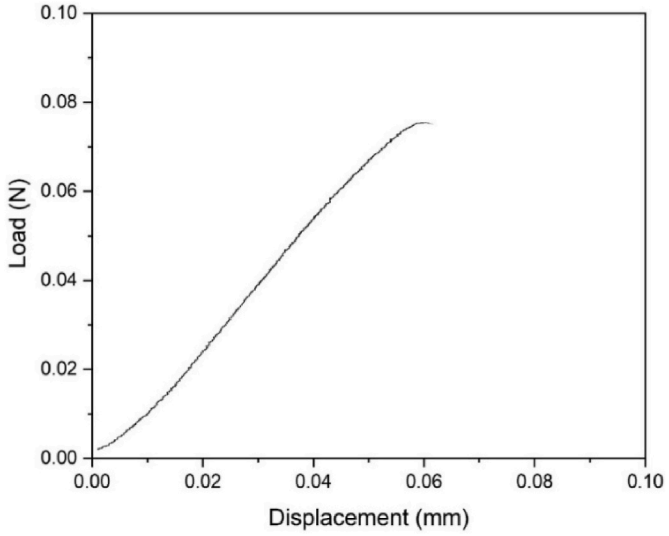

Fig. 3. Typical load-displacement curve of a successful SFPT.

amorphous region predominantly results in ductile failure mechanisms during SFPTs, opposite to crystalline polymer structures where a brittle failure mostly occurs [34].

Fig. 4 shows the maximum load, F_{max}, versus the embedded fibre length L_e and the embedded fibre area A_e. As expected, increasing the values of L_e and A_e most led to higher debonding loads. The common practice in single fibre tests is to assume a uniform shear stress distribution along the interface, enabling the calculation of the IFSS by dividing the debonding force by the interfacial area [35]. This assumption typically results in a linear correlation between the debonding force and the embedded length which is also captured in Fig. 4. Furthermore, Fig. 4 shows that the thermally treated groups have a higher slope a than the "virgin" group in all the examined temperatures and heating rates. This is indicative of the improved interfacial adhesion that occurs in these samples (Fig. 4). Altogether, Fig. 4 shows that the interfacial adhesion of CF/PEEK improves when high-temperature processing is applied, and to facilitate the comparison, the average IFSS values and standard deviations of the examined groups are presented in Fig. 5, while the results of each test are gathered in Table 1.

Fig. 5 shows that the IFSS of CF/PEEK improves upon excessive heating. In addition, at both the examined heating rates the extent of the observed improvement reduces at higher temperatures as the thermal degradation progresses. This is expected considering the increased extent of thermal damage that is induced in the material at higher temperatures. To ensure that the apparent IFSS change is statistically significant, an analysis of variance (ANOVA) takes place using a 95% confidence level (p-value <0.05). Indeed, for the five examined groups the null hypothesis is rejected (p-value $= 0.0347$) which means that there is a 95% confidence that the observed IFSS change is representative of a true change in the interface of CF/PEEK due to the applied high-temperature processing (Table 1).

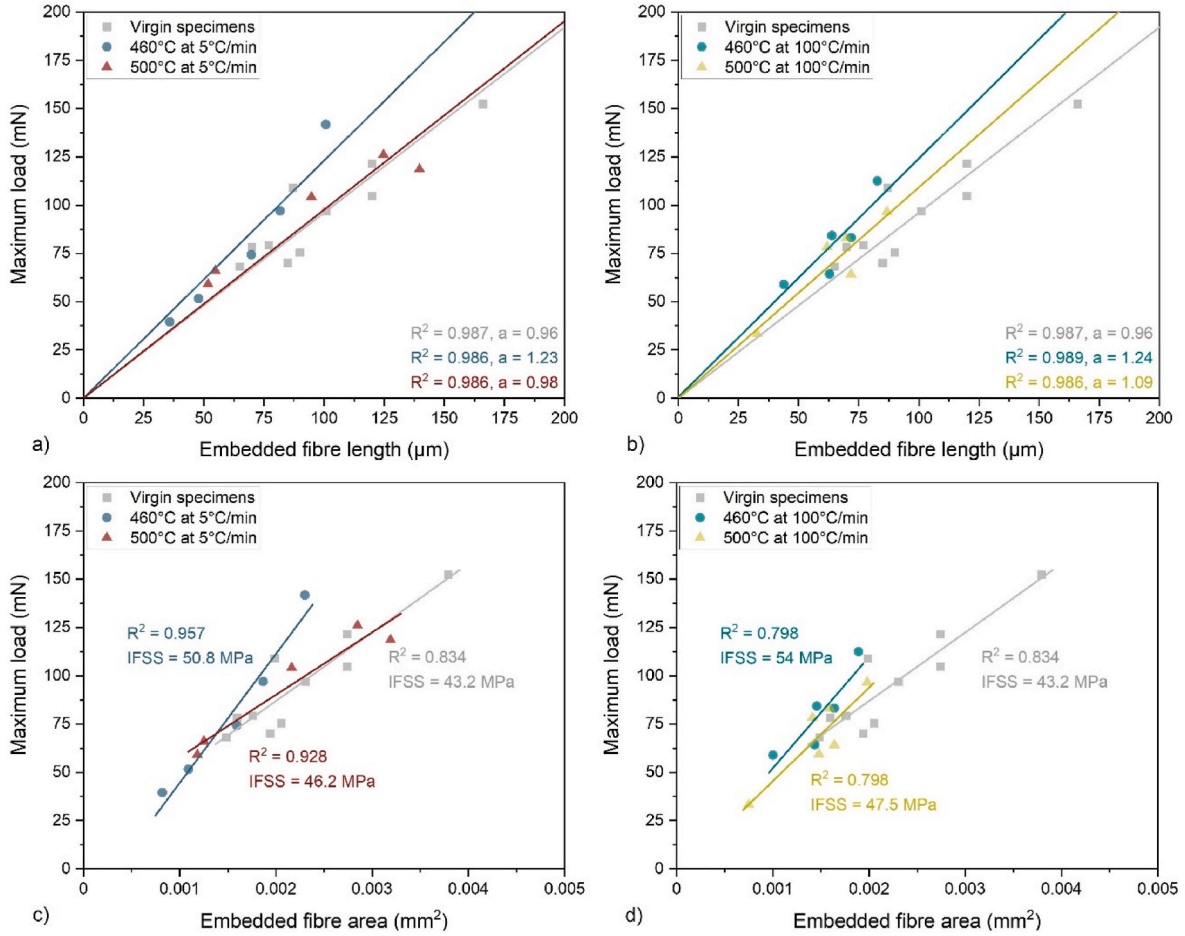

Fig. 4. Maximum load (F_{max}) versus the embedded fibre length (L_e) (a–b), and the embedded fibre area (A_e) (c–d) of the non-post treated (virgin) and the thermally treated specimens.

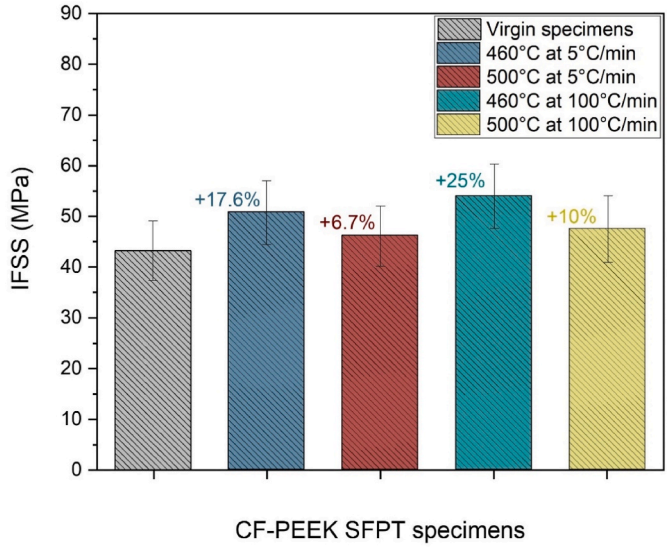

Fig. 5. IFSS of the non-post treated (virgin) and the thermally treated CF/PEEK specimens.

3.2. Observed failure modes

The main failure modes that are observed during SFPTs are fibre breakage, fibre-matrix debonding, and failure between the interfacial layer and the PEEK matrix (Fig. 6). In the latter case, the interfacial layer can have the form of a transcrystalline layer (TCL) depending on whether TC has developed. Interestingly, besides fibre breakage, different failure modes are identified in the non-post treated and the thermally treated specimens. Fibre-matrix debonding is the predominant failure mode that takes place in the non-post treated specimens, while failure between the interfacial layer and the PEEK matrix is mainly noticed after the applied rapid high-temperature processing.

Fig. 7 shows several non-treated specimens as captured with OM before and after the fibre pull out. A meniscus is identified, evident in the tested specimens of Fig. 7. This meniscus has been recently observed in other studies where untreated CF/PEEK specimens are examined with SFPTs and it indicates the occurrence of fibre-matrix debonding [2]. The failure takes place in the area close to the free fibre length which attracts the highest stresses in the single fibre composites. It initiates either with the fracture of the meniscus or at the interface between the fibre and the matrix [2]. After the onset of fracture, the fibres are successfully pulled out as soon as the applied energy triggers the complete debonding of the embedded CF from the surrounding matrix. Contrary to that, when L_e exceeds the critical fibre length (L_c) fibre breakage occurs.

On the other hand, in the thermally treated specimens, the failure is mainly observed between the interfacial layer and the PEEK matrix (Fig. 6c). For example, adhered PEEK matrix is found at the pulled fibres of the heated specimens (Fig. 8b, Fig. 8c, Fig. 9b), which indicates a strong adhesion between the fibre and the interfacial layer. In the examined specimens, the failure initiates from this area and then the fracture rapidly propagates along and in some cases across the interface region (Fig. 9a). In cases where the fracture has initiated in the vicinity of the meniscus (Fig. 9a), to ensure the accuracy of the IFSS results, the remaining meniscus size is measured and deducted from the initially measured embedded length of each fibre. This adjustment provides the effective embedded length of the fibre prior to debonding, which is then utilized to correct the IFSS value for each sample.

To further examine the failure propagation in the thermally-treated samples, the specimens of Fig. 8d and Fig. 9c - where adhered PEEK matrix is found on their pulled fibres - are also examined with SEM. The

Table 1
IFSS results of each tested specimen of the five examined groups, and summary of the ANOVA analysis.

Examined group	Resulting IFSS of each tested specimen (MPa)					Average IFSS & standard deviation (MPa)
Non-post treated (virgin)	36.11	36.63	44.98	48.91	44.33	43.2 ± 5.9
	41.96	40.17	45.87	38.17	54.86	
460 °C at 5 °C/min	46.29	47.68	46.79	61.38	51.69	50.8 ± 6.3
500 °C at 5 °C/min	37.29	47.89	49.42	52.30	44.06	46.2 ± 5.8
460 °C at 100 °C/min	50.41	58.31	44.48	59.24	57.47	54 ± 6.4
500 °C at 100 °C/min	38.80	43.65	51.67	48.46	55.08	47.5 ± 6.45

Analysis of Variance (ANOVA) summary

Source	Degrees of freedom (DF)	Sum of squares (SS)	Mean Square (MS)	F-stat	P-value
Between groups	4	456.9468	114.2367	3.0685	0.0347
Within groups	25	930.728	37.2291		
Total	29	1387.6747			

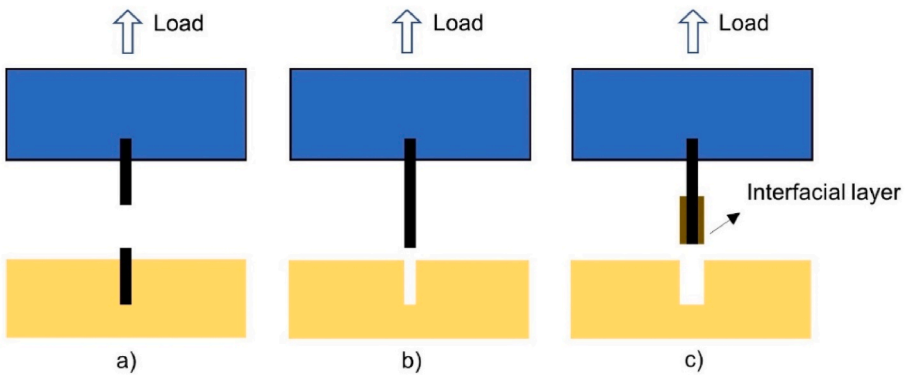

Fig. 6. Schematic of the observed failure modes in the interface of CF/PEEK during SFPTs: a) CF breakage, b) debonding at the CF/PEEK interface, and c) debonding between the interfacial layer and the PEEK matrix.

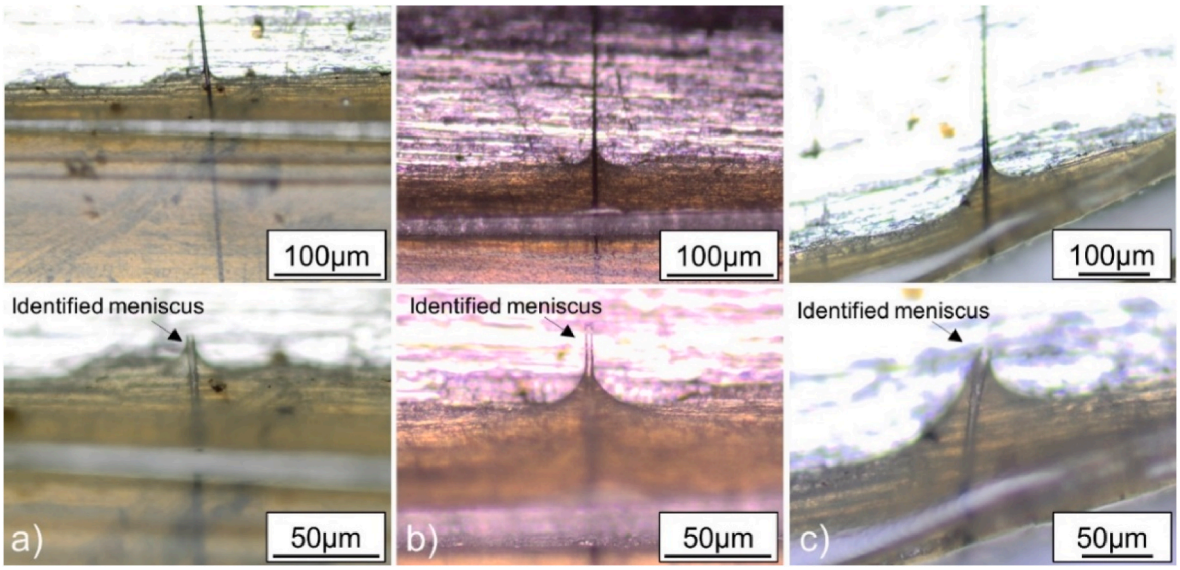

Fig. 7. Non-post treated (virgin) specimens before (top) and after SFPTs (bottom) as captured with OM.

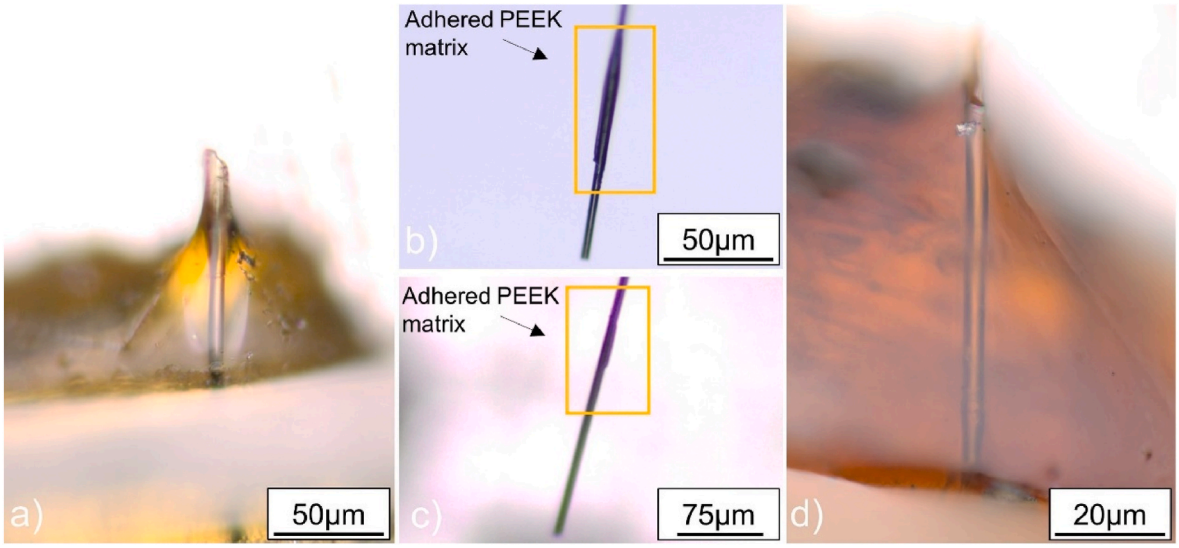

Fig. 8. Specimens heated at 5 °C/min up to: a) 460 °C, and d) 500 °C after SFPTs & their pulled-out fibres with residual interfacial layer adhered to their surface: b) 460 °C, and c) 500 °C.

SEM imaging of the treated specimens clearly captures the fracture that has taken place in the contact region between the matrix and the interfacial layer (Fig. 10). This together with the adhered PEEK matrix at the pulled fibres of those specimens indicates the strong adhesion that is established after the applied rapid high-temperature processing. Regarding the non-post treated specimens, in a recent study of Lamorinière et al. a meniscus similar to the one identified in the non-post treated samples of this work (Fig. 7) has been clearly depicted with SEM [2]. Interestingly, comparing the SEM imaging of the two studies showcases the different failure mechanisms that have taken place in the non-post treated and the thermally treated specimens of this work. The main mechanisms that can explain the difference in the failure modes and the improved IFSS properties (Fig. 5) of the thermally treated samples are the thermal residual stresses and the development of TC, and to validate these scenarios additional investigations with SEM and partly cross-polarised microscopy take place.

3.3. Surface morphology

Fig. 11 and Fig. 12 illustrate the surface of the specimens heated at 5 °C/min and 100 °C/min before and after the applied high-temperature processing. Before the applied heating process, a smooth surface is found at the PEEK matrix of the single fibre composites and thermal residual stresses are not formed during the specimen preparation process (section 2.2). On the other hand, thermal residual stresses are identified in the examined specimens after being heated up to 460 °C and 500 °C, at 5 °C/min and 100 °C/min, which are clearly illustrated by the wrinkled surfaces found in Fig. 11 and Fig. 12. Those stresses are due to the existing mismatch at the coefficient of the thermal expansion (CTE) between the CF and the PEEK matrix, which leads to a higher volumetric shrinkage in the PEEK matrix than in the CF after the applied heating [36]. This results in the formation of thermal residual stresses at the examined specimens which act as compressive stresses to the radial direction of the fibre. Their development explains the enhanced interfacial

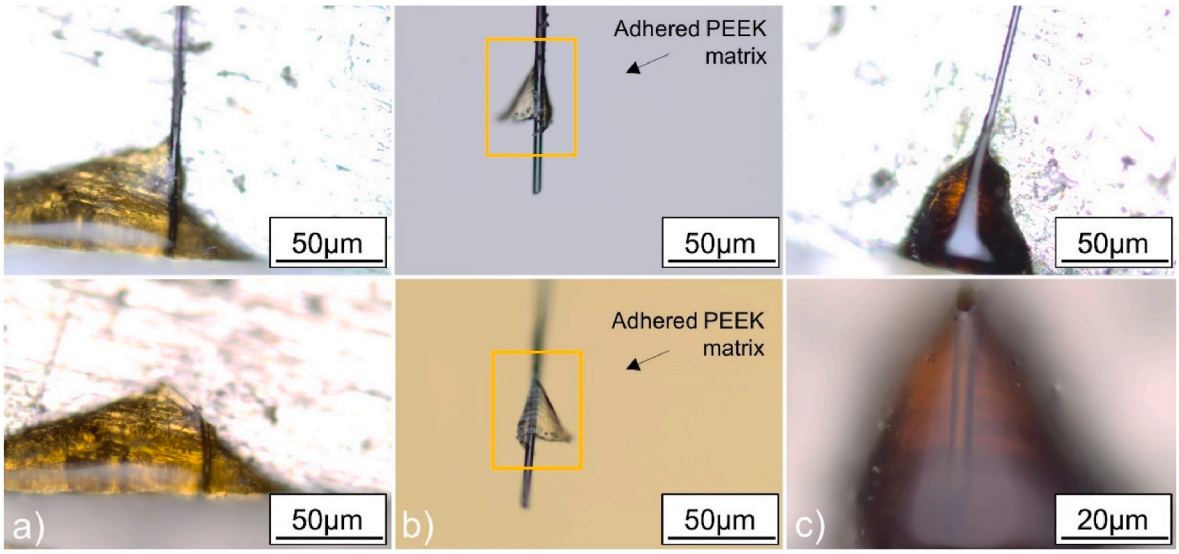

Fig. 9. Specimens heated at 100 °C/min up to: a) 460 °C, and c) 500 °C before and after SFPTs & b) pulled-out fibre of the 460 °C specimen where failure takes place along and across the interfacial layer.

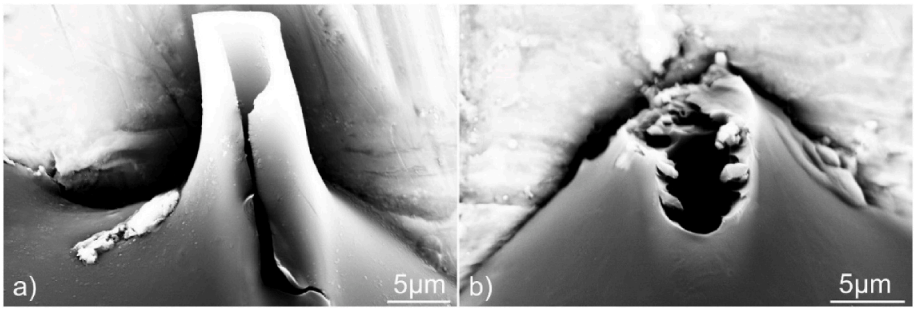

Fig. 10. Surface morphology of single CF/PEEK specimens after successful SFPTs as captured with SEM: a) 500 °C at 5 °C/min (Fig. 8d), and b) 500 °C at 100 °C/min (Fig. 9c). Indicative of the failure that has taken place between the interfacial layer and the PEEK matrix.

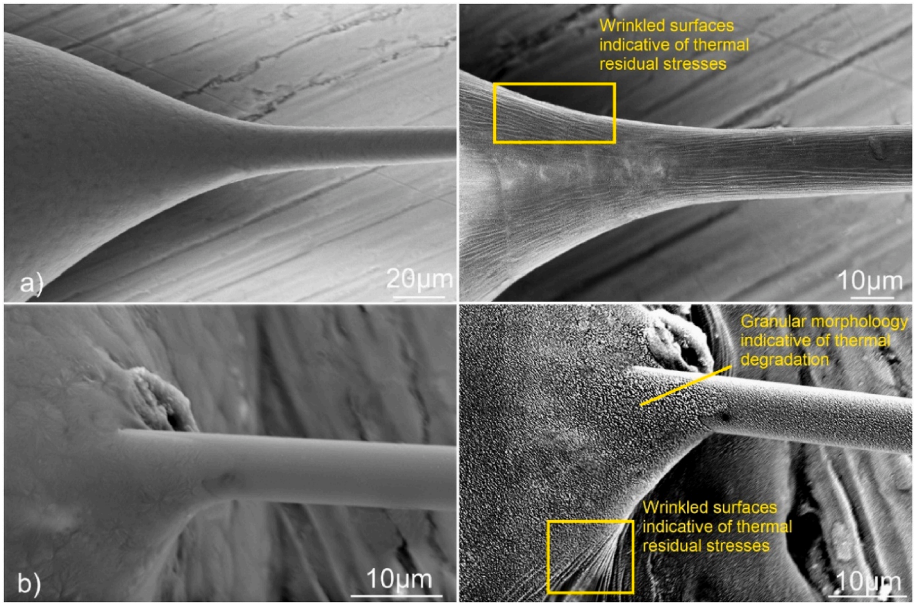

Fig. 11. Surface morphology of the single CF/PEEK specimens before and after being heated at 5 °C/min up to: a) 460 °C, and b) 500 °C (left: non-heated, right: heated) showcasing wrinkled surfaces indicative of thermal residual stresses and a granular morphology indicative of thermal degradation.

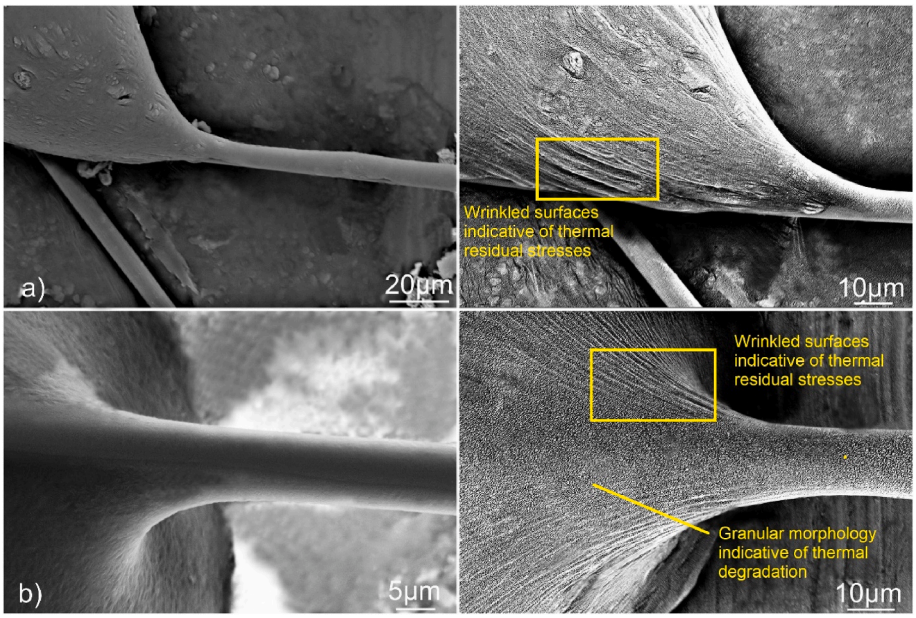

Fig. 12. Surface morphology of the single CF/PEEK specimens before and after being heated at 100 °C/min up to: a) 460 °C, and b) 500 °C (left: non-heated, right: heated) showcasing wrinkled surfaces indicative of thermal residual stresses and a granular morphology indicative of thermal degradation.

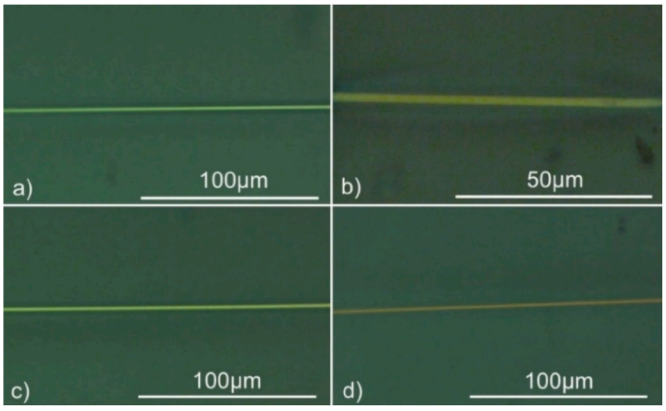

Fig. 13. Partly cross-polarised microscopy of single CF/PEEK specimens after being heated up to: a) 460 °C at 5 °C/min, b) 500 °C at 5 °C/min, c) 460 °C at 100 °C/min, and d) 500 °C at 100 °C/min.

adhesion of the thermally treated CF/PEEK specimens and the different failure modes that are observed compared to the non-post treated specimens.

The wrinkled surfaces - indicative of the formation of thermal residual stresses - are particularly evident at the samples heated at 100 °C/min (Fig. 12), which overall showed a higher increase in the IFSS compared to the samples treated at slower heating rates (Fig. 5). To a lesser extent, these wrinkled surfaces are also observed in the samples heated at 5 °C/min, indicating the presence of thermal residual stresses in these specimens as well. Nevertheless, a granular morphology was mainly identified at the PEEK matrix of the specimens treated at 5 °C/min which was more intense in the specimens heated up to 500 °C (Fig. 11b). This granular morphology is also noticed in the specimens heated at 100 °C/min up to 500 °C (Fig. 12b) and indicates the increased extent of thermal degradation that occurs at the samples when heated at elevated temperatures and at slower heating rates [13].

Altogether, the specimens heated at 5 °C/min spend significantly longer durations above the melting point of PEEK compared to those heated at 100 °C/min. For instance, specimens heated up to 500 °C at 100 °C/min remain above the T_m of PEEK for approximately 105 s, whereas at a heating rate of 5 °C/min, this dwell time increases by 20 times to approximately 2100 s or 35 min. This prolonged exposure time accelerates thermal damage in PEEK, leading to the observed granular morphology, particularly evident at higher temperatures and at slower heating rates (Fig. 11, Fig. 12). These findings are supported by a recent DSC investigation by the authors showing that slower heating rates have a greater impact on the crystallinity content of PEEK than faster heating rates [13].

To provide a more holistic overview of CF/PEEK's response in rapid high-temperature processing, the ATR-FTIR and DSC analysis of CF/PEEK in Ref. [13] revealed that samples heated at 100 °C/min up to 460 °C experienced approximately 1% degradation of their PEEK content, resulting in a 2.3% decrease in the material's degree of crystallinity (DOC) [13]. Despite this thermal damage, these conditions led to a 25% improvement in IFSS in the examined single fibre specimens of this work, with negligible effects on the crystallinity content of the bulk reinforced samples. This suggests that exposing the material to rapid heating rates up to 100 °C/min at temperatures near the onset of thermal degradation (460 °C) could potentially enhance the overall bulk material response. However, a more comprehensive study is recommended to confirm these findings, particularly examining the effect of the applied post-manufacturing tempering on other bulk material properties such as the interlaminar shear strength (ILSS), the in-plane shear, the tensile and compression, as well as the porosity content. This investigation constitutes a follow-up study by the authors.

3.4. Transcrystallinity assessment

Several studies have examined how the applied processing conditions can affect the development of transcrystallinity in CF/PEEK [29,37–41]. Overall, the temperatures that are applied during the specimens' preparation, the dwell time at these temperatures, the cooling rate, and the holding time at crystallisation temperature can affect its development [29,37,39,40]. In addition, the fibre's surface chemical and physical characteristics can impact the nucleation activity that takes place at the polymer matrix and thus influence the development of TC [42]. In general, high-modulus CFs have a relatively low surface energy that reduces the amount of interaction between the fibre's surface and the amorphous region of the PEEK matrix [29,41]. This reduced interaction favours the nucleation activity perpendicular to the fibre's

surface which under the right processing conditions could lead to the formation of TC. On the other hand, low-modulus CFs such as AS4 have a higher surface energy and tend to invite the amorphous region of the polymer, establishing an interaction that hinders the development of TC [41].

In this study, standard modulus T700SC CFs are used which have successfully developed a TCL across their interface with PEEK in previous studies [26,39], and to detect the development of TC in this work partly cross-polarised microscopy is used. Interestingly, Fig. 13 does not capture a significant spherulitic growth and the development of transcrystallinity does not occur in the examined processing conditions. Gao et al. have pointed out that a slower cooling rate enhances the formation of TC by providing the required time for the nucleation of PEEK to take place around the fibre surface [37]. On the other hand, when fast cooling is applied there is less time for the molecules of PEEK to restructure themselves in an ordered manner and around the fibre. Therefore, the fact that the specimens of this study have been naturally cooled down to room temperature with a cooling rate close to 1500 °C/min is the main reason that TC has not been formed at the examined samples.

3.5. Thermal degradation assessment: ATR-FTIR analysis

After the SFPTs, the single fibre specimens are examined with ATR-FTIR. Fig. 14a illustrates the main spectral changes that are found within the 1800 - 600 cm^{-1} spectral region. The formation of a fluorenone peak is evident at 1711 cm^{-1} and at 1452 cm^{-1}, a shoulder is detected at the proximal ether peak at 1216 cm^{-1}, and changes at the diphenylether bonds are found around 1110 cm^{-1}. Moreover, changes in the aromatic hydrogens are identified at 863 cm^{-1} and 841 cm^{-1} [11,13,43]. These spectral changes are attributed to the crosslinking mechanisms that take place in the aromatic ring of PEEK upon the event of thermal degradation. As discussed, the intensity of the 1711 cm^{-1} fluorenone peak has been associated with the progress of thermal degradation in PEEK and CF/PEEK [13]. Therefore, it is also used in this study to identify the extent of thermal degradation that takes place at the single CF/PEEK specimens at the examined heating conditions.

Fig. 14b and Fig. 14c show the average value and the standard deviation of fluorenone's intensity in the examined specimens. In addition, fluorenone's intensity is also presented when pure PEEK is heated up to a mass loss equal to 0.5%, 1.2%, and 4% at heating rates up to 100 °C/min [13]. The results show that thermal degradation of slightly less than 0.5% is induced in the single fibre composites when heated up to 460 °C at 5 °C/min and 100 °C/min. When the specimens are heated up to 500 °C, the extent of the resulting thermal degradation is around 2.3% for the two examined heating rates (Fig. 14b, Fig, 14c). Consequently, even though the thermal degradation mechanisms of PEEK are slightly triggered at 460 °C, a significantly improved IFSS is found when the

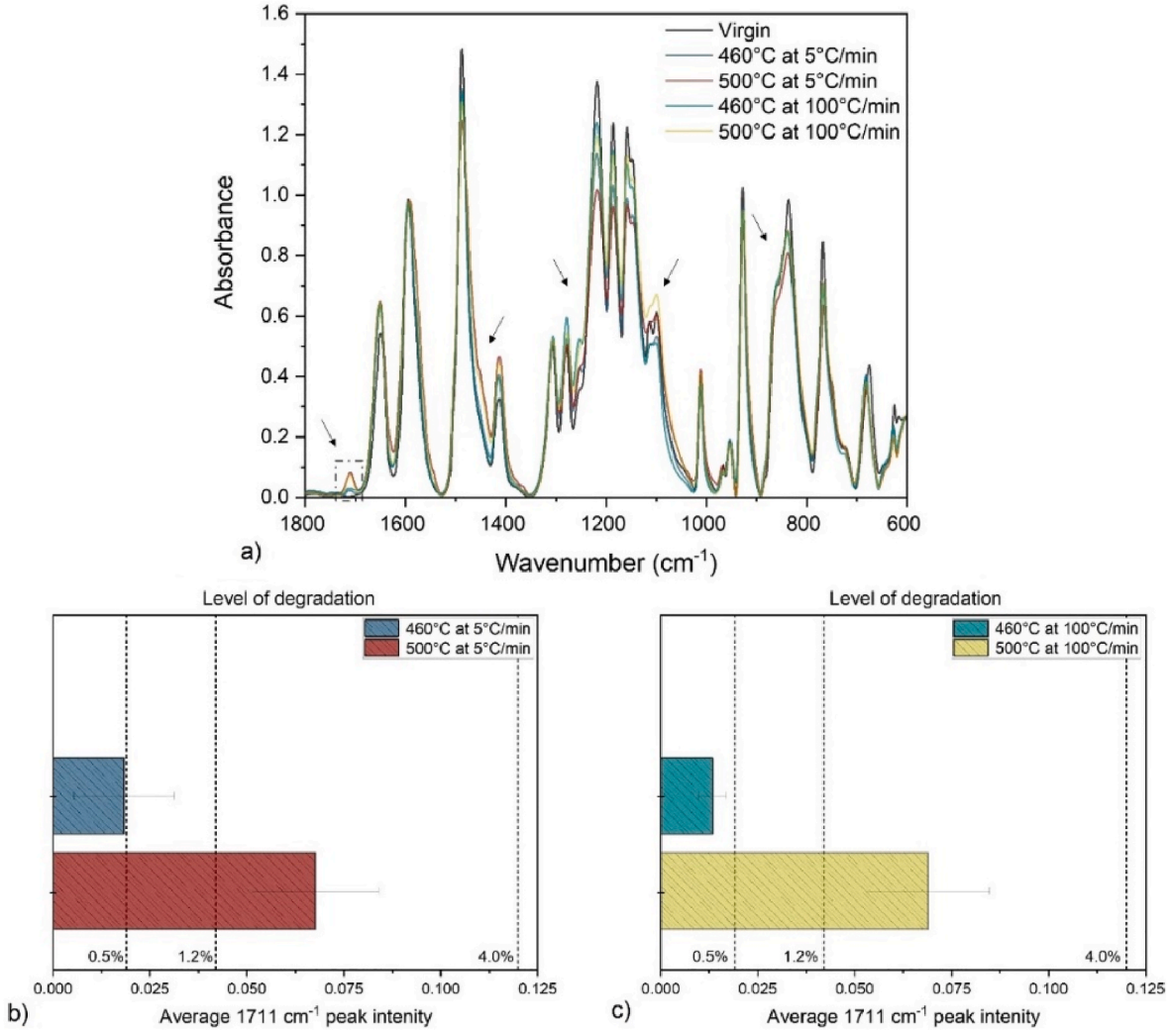

Fig. 14. a) IR spectra of the single CF/PEEK specimens at the examined heating conditions (1800 - 600 cm^{-1}) & average value and standard deviation of the intensity of the 1711 cm^{-1} peak after heating the single CF/PEEK specimens at b) 5 °C/min, and c) 100 °C/min for identifying the resulting extent of thermal degradation.

specimens are heated up to 460 °C at 5 °C/min and 100 °C/min (17.6% and 25% respectively). Interestingly, the positive effect on the IFSS is still evident at 500 °C (6.7% and 10% respectively) despite the significant amount of thermal degradation (2.3%). Therefore, the analysis highlights the significance of the formed thermal residual stresses in improving the interfacial adhesion of CF/PEEK even in cases where considerable thermal damage is induced in the material.

4. Conclusions

The micro-scale study presented herein has provided key information for understanding the response of the CF/PEEK interface at excessive heating. The results show that high-temperature processing enhances the interfacial adhesion of CF/PEEK due to the beneficial formation of thermal residual stresses. So far, several authors have suggested that the occurrence of thermal residual stresses may contribute significantly to the IFSS of CFRPs, but an actual representation of the phenomenon at the micro-scale level has not taken place. This study clearly illustrates their development and directly correlates their formation with the improved IFSS properties of the examined single fibre composites. Overall, a better response is found at faster heating rates due to the reduced thermal damage that is induced in the material at these conditions. For example, at 100 °C/min, an improved interfacial adhesion up to 25% is found at temperatures where a low-level thermal damage is induced. At higher temperatures and despite the increased thermal damage, an IFSS increase of up to 10% is still identified which demonstrates the significant impact that the formed thermal residual stresses have on the IFSS of CF/PEEK.

Considering that the interface of CF/PEEK is challenging to improve, these findings show promise. Nevertheless, to fully exploit the outcomes of this investigation it is important to associate these results with industrial manufacturing scenarios. Follow-up studies are recommended to increase our understanding in the relationship between the manufacturing processing conditions, the interface response, and their impact on the mechanical properties of bulk composites. This would further aid in identifying the appropriate methods for employing thermal residual stresses as a mechanism that could tailor the performance of the bulk CF/PEEK composites in a desired manner. For example, and especially in out-of-autoclave applications, by enhancing the interfacial adhesion of CF/PEEK, rapid high-temperature processing could be a quick and effective method for improving the structural properties of the bulk CF/PEEK composites that are associated with its interface, such as the in-plane shear strength or the interlaminar shear strength. Consequently, rapid high-temperature processing could serve to further improve the performance of thermoplastic composites, thereby enhancing their reliability and advancing their industrial use in applications currently dominated by thermosetting composites.

CRediT authorship contribution statement

Dimitrios Gaitanelis: Writing – review & editing, Writing – original draft, Visualization, Validation, Project administration, Methodology, Investigation, Formal analysis, Data curation, Conceptualization. **Chris Worrall:** Writing – review & editing, Supervision, Resources, Project administration. **Mihalis Kazilas:** Supervision, Resources, Project administration, Funding acquisition.

Declaration of competing interest

The authors declare that they have no known competing financial interests or personal relationships that could have appeared to influence the work reported in this paper.

Data availability

Data will be made available on request.

Acknowledgement

This publication was made possible by the sponsorship and support of TWI. The work was enabled through, and undertaken at, the National Structural Integrity Research Centre (NSIRC), a postgraduate engineering facility for industry-led research into structural integrity established and managed by TWI through a network of both national and international Universities.

We would also like to thank Dr Angeliki Chanteli for her helpful comments.

References

[1] P. Kiss, W. Stadlbauer, C. Burgstaller, H. Stadler, S. Fehringer, F. Haeuserer, V.-M. Archodoulaki, In-house recycling of carbon- and glass fibre-reinforced thermoplastic composite laminate waste into high-performance sheet materials, Compos Part A Appl Sci Manuf 139 (2020) 106–110, https://doi.org/10.1016/j.compositesa.2020.106110.

[2] S. Lamorinière, M.P. Jones, K. Ho, G. Kalinka, M.S.P. Shaffer, A. Bismarck, Carbon nanotube enhanced carbon Fibre-Poly(ether ether ketone) interfaces in model hierarchical composites, Compos. Sci. Technol. 221 (2022), https://doi.org/10.1016/j.compscitech.2022.109327.

[3] P. Patel, T.R. Hull, R.E. Lyon, S.I. Stoliarov, R.N. Walters, S. Crowley, N. Safronava, Investigation of the thermal decomposition and flammability of PEEK and its carbon and glass-fibre composites, Polym. Degrad. Stabil. 96 (2011) 12–22, https://doi.org/10.1016/j.polymdegradstab.2010.11.009.

[4] C.M. Stokes-Griffin, P. Compston, An inverse model for optimisation of laser heat flux distributions in an automated laser tape placement process for carbon-fibre/PEEK, Compos Part A Appl Sci Manuf 88 (2016) 190–197, https://doi.org/10.1016/j.compositesa.2016.05.034.

[5] D. Peeters, G. Clancy, V. Oliveri, R. O'Higgins, D. Jones, P.M. Weaver, Concurrent design and manufacture of a thermoplastic composite stiffener, Compos. Struct. 212 (2019) 271–280, https://doi.org/10.1016/j.compstruct.2019.01.033.

[6] A.K. Bandaru, G. Clancy, D. Peeters, R.M. O'Higgins, P.M. Weaver, Properties of a thermoplastic composite skin-stiffener interface in a stiffened structure manufactured by laser-assisted tape placement with in situ consolidation, Compos. Struct. 214 (2019) 123–131, https://doi.org/10.1016/j.compstruct.2019.02.011.

[7] A.J. Comer, D. Ray, W.O. Obande, D. Jones, J. Lyons, I. Rosca, R.M. O' Higgins, M. A. McCarthy, Mechanical characterisation of carbon fibre–PEEK manufactured by laser-assisted automated-tape-placement and autoclave, Compos Part A Appl Sci Manuf 69 (2015) 10–20, https://doi.org/10.1016/j.compositesa.2014.10.003.

[8] D. Wu, Q. Miao, Z. Dai, F. Niu, G. Ma, Effect of voids and crystallinity on the interlaminar shear strength of in-situ manufactured CF/PEEK laminates using repass treatment, Compos. Sci. Technol. 224 (2022) 109448, https://doi.org/10.1016/j.compscitech.2022.109448.

[9] A.R. Chadwick, K. Kotzur, S. Nowotny, Moderation of thermoplastic composite crystallinity and mechanical properties through in situ manufacturing and post-manufacturing tempering: Part 1 – mechanical characterisation, Compos Part A Appl Sci Manuf 143 (2021) 106286, https://doi.org/10.1016/j.compositesa.2021.106286.

[10] K. Kotzur, A.R. Chadwick, M. Löbbecke, Moderation of thermoplastic composite crystallinity and mechanical properties through in-situ manufacturing and post-manufacturing tempering: Part 2 – morphological characterisation, Compos Part A Appl Sci Manuf 163 (2022) 107225, https://doi.org/10.1016/j.compositesa.2022.107225.

[11] D. Gaitanelis, A. Chanteli, C. Worrall, P.M. Weaver, M. Kazilas, A multi-technique and multi-scale analysis of the thermal degradation of PEEK in laser heating, Polym. Degrad. Stabil. 211 (2023) 110282, https://doi.org/10.1016/j.polymdegradstab.2023.110282.

[12] A. Chanteli, A.K. Bandaru, D. Peeters, R.M. O'Higgins, P.M. Weaver, Influence of repass treatment on carbon fibre-reinforced PEEK composites manufactured using laser-assisted automatic tape placement, Compos. Struct. 248 (2020), https://doi.org/10.1016/j.compstruct.2020.112539.

[13] D. Gaitanelis, C. Worrall, M. Kazilas, Detecting, characterising and assessing PEEK's and CF-PEEK's thermal degradation in rapid high-temperature processing, Polym. Degrad. Stabil. 204 (2022) 110096, https://doi.org/10.1016/j.polymdegradstab.2022.110096.

[14] S. Zhandarov, E. Mäder, Characterization of fiber matrix interface strength applicability of different tests, approaches and parameters, Compos. Sci. Technol. 65 (2005) 149–160, https://doi.org/10.1016/j.compscitech.2004.07.003.

[15] L. Yang, J.L. Thomason, W. Zhu, The influence of thermo-oxidative degradation on the measured interface strength of glass fibre-polypropylene, Compos Part A Appl Sci Manuf 42 (2011) 1293–1300, https://doi.org/10.1016/j.compositesa.2011.05.011.

[16] L.T. Drzal, M.J. Rich, P.F. Lloyd, Adhesion of graphite fibers to epoxy matrices: I. The role of fiber surface treatment, J. Adhes. 16 (1983) 1–30, https://doi.org/10.1080/00218468308074901.

[17] Y. Su, P. Liu, D. Jing, X. Zhang, S. Zhang, Improved interfacial adhesion in carbon fiber/poly (ether ether ketone) composites with the sulfonated poly (ether ether ketone) sizing treatment, J. Appl. Polym. Sci. 138 (2021), https://doi.org/10.1002/app.51326.

[18] S. Wang, Y. Yang, Y. Mu, J. Shi, X. Cong, J. Luan, G. Wang, Synergy of electrochemical grafting and crosslinkable crystalline sizing agent to enhance the interfacial strength of carbon fiber/PEEK composites, Compos. Sci. Technol. 203 (2021), https://doi.org/10.1016/j.compscitech.2020.108562.
[19] Y. Yang, T. Wang, S. Wang, X. Cong, S. Zhang, M. Zhang, J. Luan, G. Wang, Strong interface construction of carbon fiber–reinforced PEEK composites: an efficient method for modifying carbon fiber with crystalline PEEK, Macromol. Rapid Commun. 41 (2020), https://doi.org/10.1002/marc.202000001.
[20] T. Yan, F. Yan, S. Li, M. Li, Y. Liu, M. Zhang, L. Jin, L. Shang, L. Liu, Y. Ao, Interfacial enhancement of CF/PEEK composites by modifying water-based PEEK-NH$_2$ sizing agent, Compos. B Eng. 199 (2020), https://doi.org/10.1016/j.compositesb.2020.108258.
[21] T. Wang, Y. Jiao, Z. Mi, C. Wang, D. Wang, X. Zhao, H. Zhou, C. Chen, Improving the interfacial adhesion of carbon fiber/polyether ether ketone composites by polyimide coating, ChemistrySelect 5 (2020) 5507–5514, https://doi.org/10.1002/slct.202001232.
[22] X. Wang, Z. Huang, M. Lai, L. Jiang, Y. Zhang, H. Zhou, Highly enhancing the interfacial strength of CF/PEEK composites by introducing PAIK onto diazonium functionalized carbon fibers, Appl. Surf. Sci. 510 (2020), https://doi.org/10.1016/j.apsusc.2020.145400.
[23] J. Chen, K. Wang, Y. Zhao, Enhanced interfacial interactions of carbon fiber reinforced PEEK composites by regulating PEI and graphene oxide complex sizing at the interface, Compos. Sci. Technol. 154 (2018) 175–186, https://doi.org/10.1016/j.compscitech.2017.11.005.
[24] H. Lyu, N. Jiang, Y. Li, H. Lee, D. Zhang, Enhanced interfacial and mechanical properties of carbon fiber/PEEK composites by hydroxylated PEEK and carbon nanotubes, Compos Part A Appl Sci Manuf 145 (2021) 106364, https://doi.org/10.1016/j.compositesa.2021.106364.
[25] M. Lai, L. Jiang, X. Wang, H. Zhou, Z. Huang, H. Zhou, Effects of multi-walled carbon nanotube/graphene oxide-based sizing on interfacial and tribological properties of continuous carbon fiber/poly(ether ether ketone) composites, Mater. Chem. Phys. 276 (2022) 125344, https://doi.org/10.1016/j.matchemphys.2021.125344.
[26] N. Li, J. Chen, H. Liu, A. Dong, K. Wang, Y. Zhao, Effect of preheat treatment on carbon fiber surface properties and fiber/PEEK interfacial behavior, Polym. Compos. 40 (2019) E1407–E1415, https://doi.org/10.1002/pc.25020.
[27] M. Doumeng, L. Makhlouf, F. Berthet, O. Marsan, K. Delbé, J. Denape, F. Chabert, A comparative study of the crystallinity of polyetheretherketone by using density, DSC, XRD, and Raman spectroscopy techniques, Polym. Test. 93 (2021) 106878, https://doi.org/10.1016/j.polymertesting.2020.106878.
[28] L. Yang, J.L. Thomason, Interface strength in glass fibre–polypropylene measured using the fibre pull-out and microbond methods, Compos Part A Appl Sci Manuf 41 (2010) 1077–1083, https://doi.org/10.1016/j.compositesa.2009.10.005.
[29] H. Pérez-Martín, P. Mackenzie, A. Baidak, C.M. Ó Brádaigh, D. Ray, Crystallinity studies of PEKK and carbon fibre/PEKK composites: a review, Compos. B Eng. 223 (2021) 109–127, https://doi.org/10.1016/j.compositesb.2021.109127.
[30] D. Ray, A.J. Comer, J. Lyons, W. Obande, D. Jones, R.M.O. Higgins, M. A. McCarthy, Fracture toughness of carbon fiber/polyether ether ketone composites manufactured by autoclave and laser-assisted automated tape placement, J. Appl. Polym. Sci. 132 (2015), https://doi.org/10.1002/app.41643.
[31] C.M. Pistor, S.I. Güçeri, Crystallinity of on-line consolidated thermoplastic composites, J. Compos. Mater. 33 (1999) 306–324.
[32] C. Marotzke, The elastic stress field arising in the single-fiber pull-out test, Compos. Sci. Technol. 50 (1994) 393–405, https://doi.org/10.1016/0266-3538(94)90027-2.
[33] S. Meretz, W. Auersch, C. Marotzke, E. Schulz, A. Hampe, Investigation of morphology-dependent fracture behaviour with the single-fibre pull-out test, Compos. Sci. Technol. 48 (1993) 285–290, https://doi.org/10.1016/0266-3538(93)90145-7.
[34] T. Ramanathan, A. Bismarck, E. Schulz, K. Subramanian, The use of a single-fibre pull-out test to investigate the influence of acidic and basic surface groups on carbon fibres on the adhesion to poly(phenylene sulfide) and matrix-morphology-dependent fracture behaviour, Compos. Sci. Technol. 61 (2001) 1703–1710, https://doi.org/10.1016/S0266-3538(01)00069-0.
[35] R.J. Day, J.V.C. Rodrigez, Investigation of the micromechanics of the microbond test, Compos. Sci. Technol. 58 (1998) 907–914, https://doi.org/10.1016/S0266-3538(97)00197-8.
[36] P.P. Parlevliet, H.E.N. Bersee, A. Beukers, Residual stresses in thermoplastic composites—a study of the literature—Part I: formation of residual stresses, Compos Part A Appl Sci Manuf 37 (2006) 1847–1857, https://doi.org/10.1016/j.compositesa.2005.12.025.
[37] S.-L. Gao, J.-K. Kim, Cooling rate influences in carbon fibre/PEEK composites. Part 1. Crystallinity and interface adhesion, Compos Part A Appl Sci Manuf 31 (2000) 517–530, https://doi.org/10.1016/S1359-835X(00)00009-9.
[38] H. Kobayashi, E. Hayakawa, T. Kikutani, A. Takaku, Effect of quenching and annealing on fiber pull-out from crystalline polymer matrices, Adv. Compos. Mater. 1 (1991) 155–168, https://doi.org/10.1163/156855191X00252.
[39] A. Beehag, L. Ye, Fibre/matrix adhesion in thermoplastic composite: is transcrystallinity a key?, in: Proceedings of ICCM–11 Gold Coast, Australia, 1997, pp. IV 723–730, 14th-18th July 1997.
[40] H. Quan, Z.-M. Li, M.-B. Yang, R. Huang, On transcrystallinity in semi-crystalline polymer composites, Compos. Sci. Technol. 65 (2005) 999–1021, https://doi.org/10.1016/j.compscitech.2004.11.015.
[41] A. Lustiger, Morphological aspects of the interface in the PEEK-Carbon Fiber system, Polym. Compos. 13 (1992) 408–412, https://doi.org/10.1002/pc.750130511.
[42] N. Ning, S. Fu, W. Zhang, F. Chen, K. Wang, H. Deng, Q. Zhang, Q. Fu, Realizing the enhancement of interfacial interaction in semicrystalline polymer/filler composites via interfacial crystallization, Prog. Polym. Sci. 37 (2012) 1425–1455, https://doi.org/10.1016/j.progpolymsci.2011.12.005.
[43] D. Gaitanelis, C. Worrall, M. Kazilas, A numerical model to prevent the thermal degradation of CFRPs at extreme heating rates – the laser processing of CF/PEEK, Compos Part A Appl Sci Manuf 177 (2024) 107938, https://doi.org/10.1016/j.compositesa.2023.107938.